Supporting Information

Induced Magnetic Field in sp-Hybridized Carbon Rings: Analysis of Double Aromaticity and Antiaromaticity in Cyclo[2n]carbon Allotropes

Nickolas D. Charistos*[a] and Alvaro Muñoz-Castro*[b]

[a]Aristotle University of Thessaloniki, Department of Chemistry, Laboratory of Quantum and Computational Chemistry, Thessaloniki, Greece, 54 124.

[b]Laboratorio de Química Inorgánica y Materiales Moleculares, Facultad de Ingeniería, Universidad Autonoma de Chile, Llano Subercaceaux 2801, San Miguel, Santiago, Chile.

Table of contents Page

Benchmarking of C_{18} geometry

A number of different exchange–correlation functionals (XC), including generalized gradient approximation (GGA), meta-GGA, hybrid, meta-hybrid and range-separated hybrid functionals, were tested for the optimization of C_{18}. The bond lengths of the optimized C_{18} structures are presented in Table S1. Among them, the following functionals with high percentage of HF exchange (HFX≥50%) produced polyynic geometries with altering bond lengths: BHandHLYP, KMLYP,[1] CAM-B3LYP,[2] MO6-HF,[3] M06-2X,[4] ωB97X[5] and ωB97XD. All other functionals with lower HFX percentage and pure GGAs that were tested, namely BP86,[6] PBE, PW91,[7] B3LYP,[8] PBE0,[9] HSE06,[10] M06L,[4] MN12-SX,[11] TPSS[12] and TPSSh[13] produced cumulenic geometries with equal bond lengths. All optimizations were performed with Slater-type triple-ζ basis set with two polarization functions (TZ2P) with the ADF code, except for ωB97XD functional which was used with 6-311++G(d,p) basis set employing Gaussian software.

Table S1. Bond lengths and bond length alternation of C_{18} computed with various functionals.

Functional	HFX	d_1 (Å)	d_2 (Å)	BLA
GGA				
BP86	0	1.283		0.000
PBE	0	1.283		0.000
PW91	0	1.282		0.000
Meta-GGA				
MO6L	0	1.274		0.000
TPSS	0	1.281		0.000
Hybrid				
B3LYP	20	1.277		0.000
KMLYP	55.7	1.336	1.207	0.129
BHandHLYP	50	1.339	1.212	0.127
PBE0	25	1.281	1.269	0.012
Meta-hybrid				
M06-2X	54	1.346	1.223	0.123
MO6-HF	100	1.375	1.207	0.168
TPSSH	10	1.277		0.000
Range-separated hybrid				
CAM-B3LYP	19-65	1.341	1.217	0.124
HSE06	25-0	1.275		0.000
MN12-SX	25-0	1.272		0.000
wb97x	15.8-100	1.359	1.212	0.147
wb97xd	22.2-100	1.346	1.223	0.123

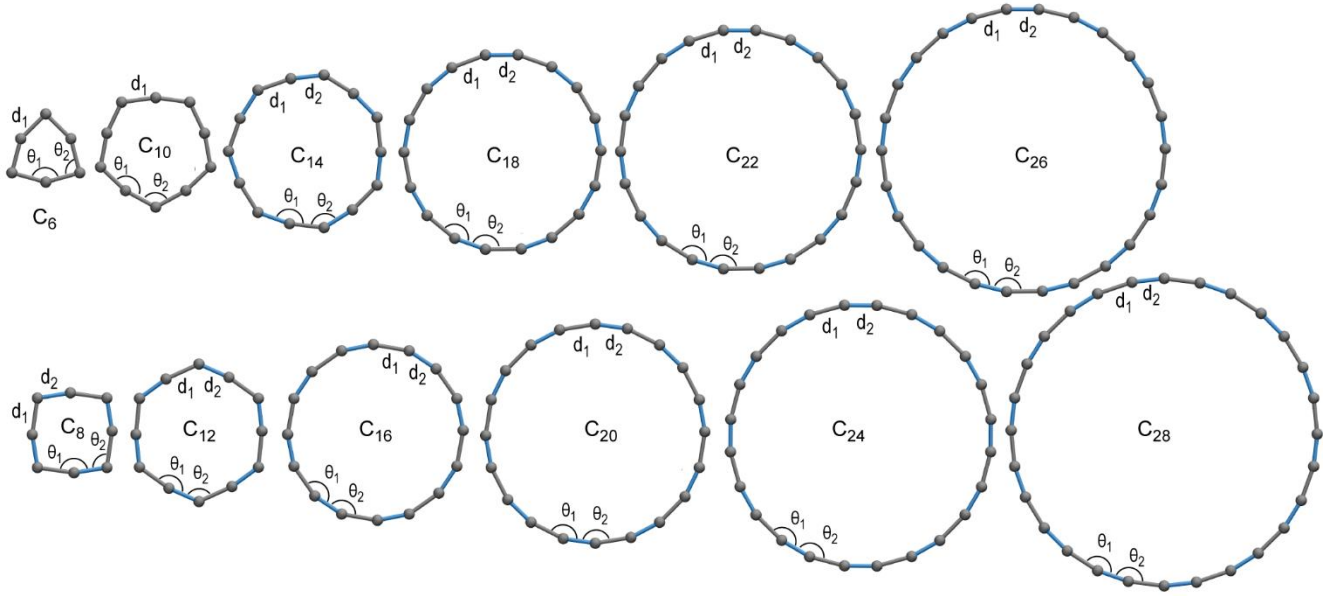

Figure S1. Optimized geometries of ground states of C_{4n+2} (n=1-6) (top) and C_{4n} (n=2-7) (bottom) carbon rings computed at the ωB97XD/6-311++G(d,p) level. Blue shades depict short bonds.

Benchmarking of NICS

$NICS_{zz}$ values at the center of each ring were calculated using PBE, B3LYP, CAM-B3LYP, wB97X-D, BHandHLYP and KMLYP functionals (Table S2, Figures S2-S3). All calculations were performed with TZ2P slater basis set using ADF, except for CAM-B3LYP and ωB97X-D which were performed with 6-311++G(d,p) gaussian basis set with Gaussian09. All functionals produce the same qualitative trends of $NICS_{zz}$ values with regard to ring size and bonding pattern, but there are significant quantitative differences among different types of functionals, except for small cumulenic rings C_6 and C_{10}. Pure GGA PBE overestimates $NICS_{zz}$ producing significant larger values with regard to other functionals. Hybrid GGAs with high HF exchange (≥50%) BHandHLYP and KMLYP and range-separated hybrid CAM-B3LYP and ωB97X-D produce almost identical $NICS_{zz}$, which is significantly smaller than PBE. Hybrid-GGA with small HF exchange (20%) B3LYP produce intermediate $NICS_{zz}$ values with regard to PBE and BHandHLYP for polyynic geometries, whereas it produces identical results with PBE for cumulenic transition states. The discrepancy between high HF exchange and low (or zero) HF exchange functionals is smaller in cumulenic geometries with regard to polyynic geometries, whereas dissection to π_{out} and π_{in} contributions reveals that PBE performs equivalent to BHandHLYP for the former and overestimates the response of the later (Figure S3). Hence the choice of functional for the quantitative measurement of the magnetic response is sensitive to the bonding pattern, where polyynic structures are more accurately modelled by high HF exchange hybrid functionals, whereas cumulenic geometries are effectively described by pure GGAs and low HF exchange hybrids. However, although PBE and B3LYP overestimate the magnetic response of polyynic structures, they accurately reproduce the qualitative features of the magnetic response with regard to the ring size and bonding pattern of C_{2N} rings

Table S2. Total $NICS_{zz}$ (ppm) calculated at ring centers with various functionals.

Molecule	PBE	B3LYP	BHandHLYP	KMLYP	CAM-B3LYP	ωB97X-D
C_6	-30.8	-33.9	-37.7	-37.7	-33.4	-33.5
C_8	157.6	147.2	130.9	130.6	131.7	135.2
C_{10}	-67.7	-66.9	-65.2	-65.9	-67.8	-68.3
C_{12}	153.9	128.8	96.8	94.9	98.2	98.5
C_{14}	-92.4	-89.3	-81.6	-81.5	-83.2	-83.0
C_{14}TS	-96.2	-94.4	-89.2	-89.6	-89.0	-89.0
C_{16}	112.1	86.5	57.9	54.9	56.4	53.9
C_{18}	-68.4	-57.2	-44.7	-40.9	-40.2	-38.4
C_{18} TS	-110.7	-109.3	-101.5	-101.1	-101.4	-100.1
C_{20}	81.5	57.4	33.4	31.0	32.4	29.4
C_{22}	-50.7	-36.9	-22.0	-19.6	-20.2	-18.3
C_{22} TS	-116.6	-115.6	-104.0	-102.2	-104.4	-99.9
C_{24}	57.1	36.6	18.6	16.9	17.9	15.4
C_{26}	-37.2	-23.4	-10.9	-9.5	-9.8	-8.5
C_{26} TS	-119.3	-118.3	-99.3	-95.0	-100.7	-89.9
C_{28}	40.0	23.3	10.5	9.4	10.0	8.0

Table S3. Dissected $NICS_{zz}$ values (ppm) computed at the PBE functional.

Molecule	Point Group	π-out	π-in	HOMO-out	HOMO-in
C_6	D_{3h}	-38.7	21.0	-24.5	39.3
C_8	C_{4h}	138.0	31.7	173.1	46.1
C_{10}	D_{5h}	-51.5	-8.3	-19.1	21.1
C_{12}	C_{6h}	107.6	51.3	151.7	87.8
C_{14}	C_{7h}	-53.4	-35.0	-11.8	5.6
C_{14}TS	D_{7h}	-56.9	-35.3	-15.1	5.2
C_{16}	C_{8h}	55.3	60.2	101.7	105.5
C_{18}	C_{9h}	-34.5	-31.0	10.7	14.3
C_{18} TS	D_{9h}	-59.4	-48.7	-12.2	-2.1
$C_{18}H_{18}$	D_{6h}	-46.7	-	-5.9	-
$C_{18}H_6$	D_{3h}	-24.9	16.3	14.7	35.1
C_{20}	C_{10h}	40.2	43.6	87.6	90.2
C_{22}	C_{11h}	-25.6	-23.0	21.7	24.3
C_{22} TS	D_{11h}	-60.7	-54.0	-10.2	-4.0
C_{24}	C_{12h}	28.3	30.6	75.1	76.8
C_{26}	C_{13h}	-18.8	-16.8	29.6	31.5
C_{26} TS	D_{13h}	-61.4	-56.3	-8.7	-4.1
C_{28}	C_{14h}	19.9	21.5	65.4	66.5

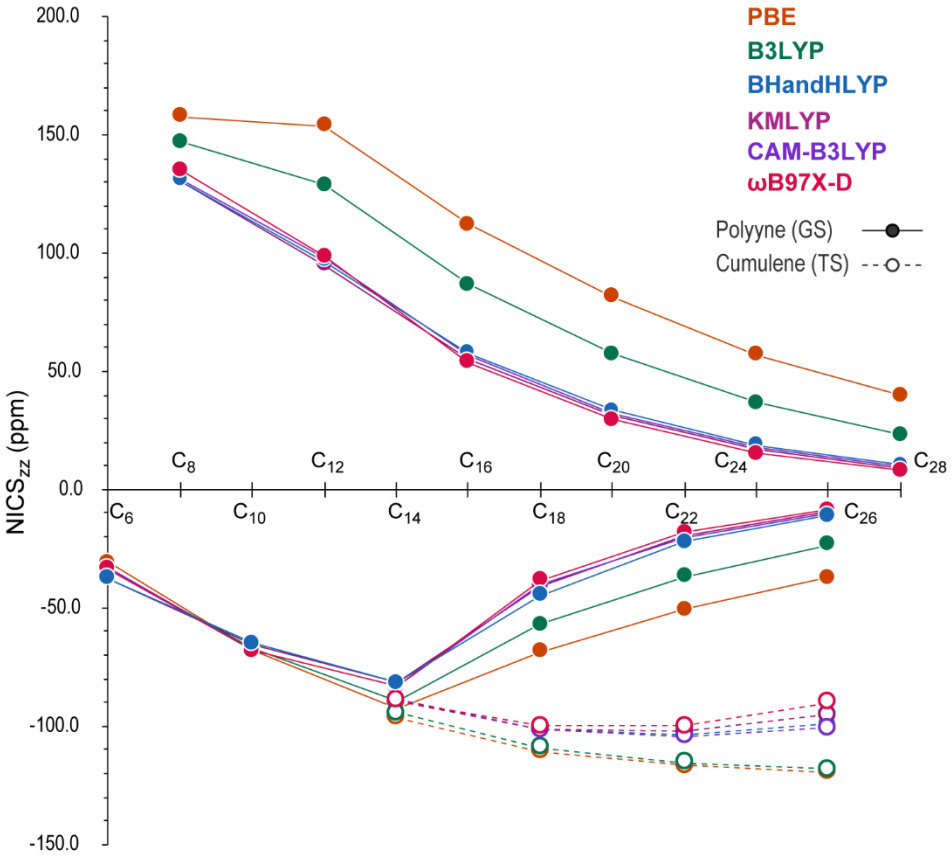

Figure S2. $NICS_{zz}$ trends with regard to ring size and molecular geometry of C_{2N} (N=3-14) molecules computed with different functionals.

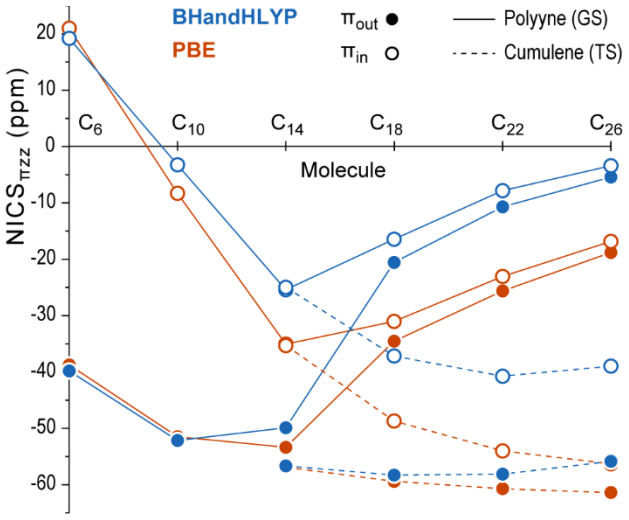

Figure S3. Dissected π_{out} and π_{in} NICSzz trends with regard to ring size and molecular geometry of C_{4n+2} (n=1-6) molecules computed with PBE and BHandHLYP functionals.

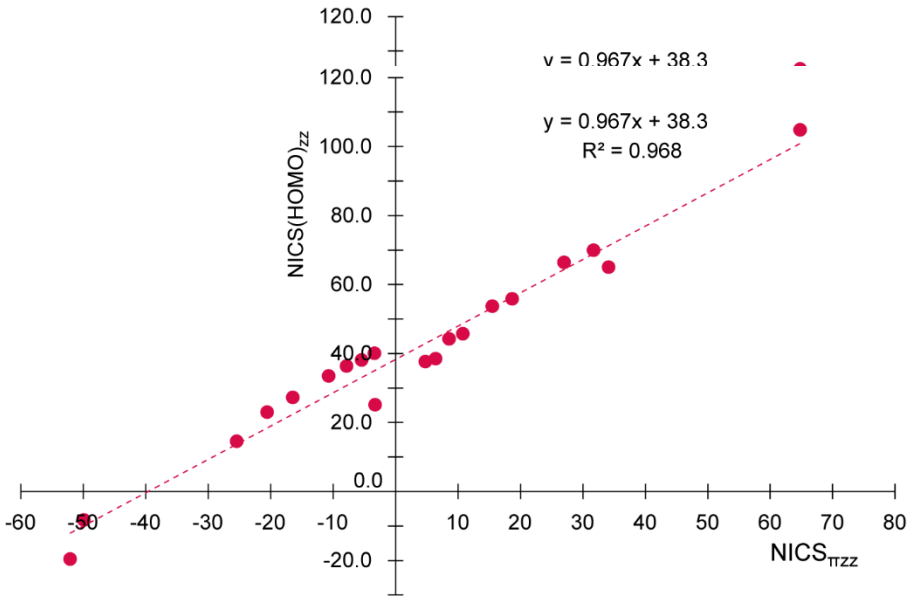

Figure S4. Linear correlation of $HOMO_{out}$ and $HOMO_{in}$ contributions to $NICS_{zz}$ with regard to π_{out} and π_{in} contributions to $NICS_{zz}$ of ground states C_{2N} (N=5-14).

Table S4. Energy gaps of frontier π_{out} and π_{in} orbitals (eV) and contributions of $HOMO_{out}$ and $HOMO_{in}$ to $NICS_{zz}$ (ppm) computed with BHandHLYP functional.

Molecule	Gap_{out}	Gap_{in}	$NICS_{zz}$ $HOMO_{out}$	$NICS_{zz}$ $HOMO_{in}$	Molecule	Gap_{out}	Gap_{in}	$NICS_{zz}$ $HOMO_{out}$	$NICS_{zz}$ $HOMO_{in}$
C_6			-25.5	36.0	C_8			144.1	40.5
C_{10}	7.32	7.78	-19.6	25.2	C_{12}	4.51	5.43	104.8	65.0
C_{14}	5.72	5.89	-8.3	14.6	C_{16}	4.53	4.48	66.4	70.0
C_{14} TS	5.66	5.90	-14.6	14.3	C_{20}	4.34	4.31	53.7	55.9
C_{18}	5.43	5.34	23.0	27.3	C_{24}	4.25	4.23	44.3	45.7
C_{18} TS	4.53	4.73	-10.9	8.6	C_{28}	4.20	4.19	37.7	38.5
C_{22}	5.11	5.06	33.5	36.3					
C_{22} TS	3.84	4.02	-7.4	8.7					
C_{26}	4.88	4.85	38.2	40.1					
C_{26} TS	3.37	3.56	-3.0	12.5					

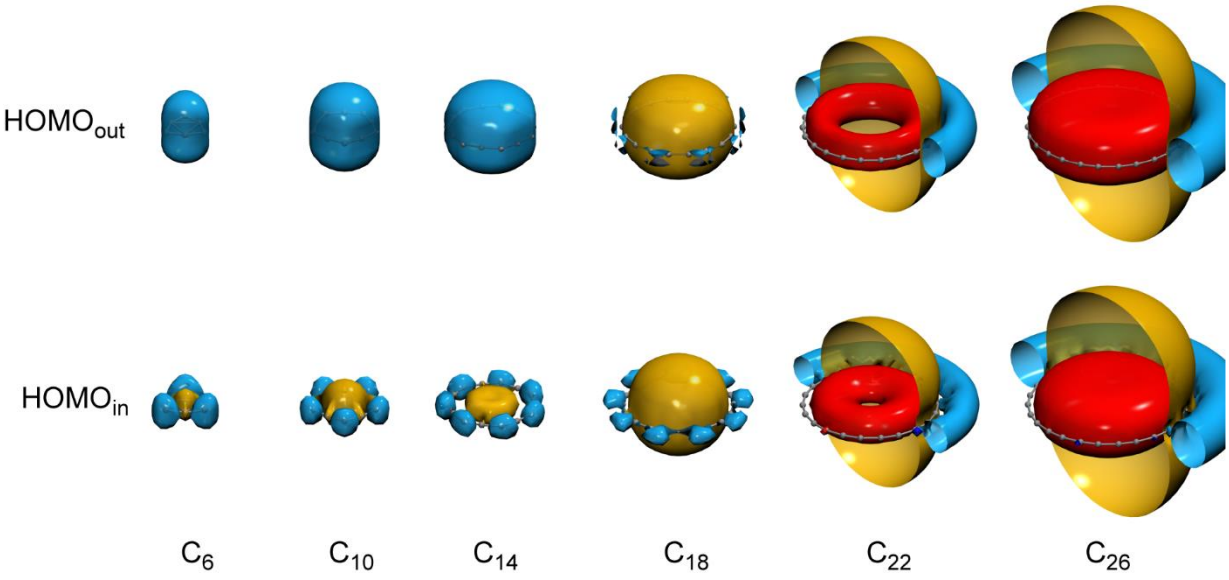

Figure S5. Isosurfaces of $HOMO_{out}$ (top) and $HOMO_{in}$ (bottom) contributions to B_z^{ind} of ground states C_{4n+2} (n=1-6) rings. Isovalues: cyan -5ppm, orange +5ppm, red +25ppm.

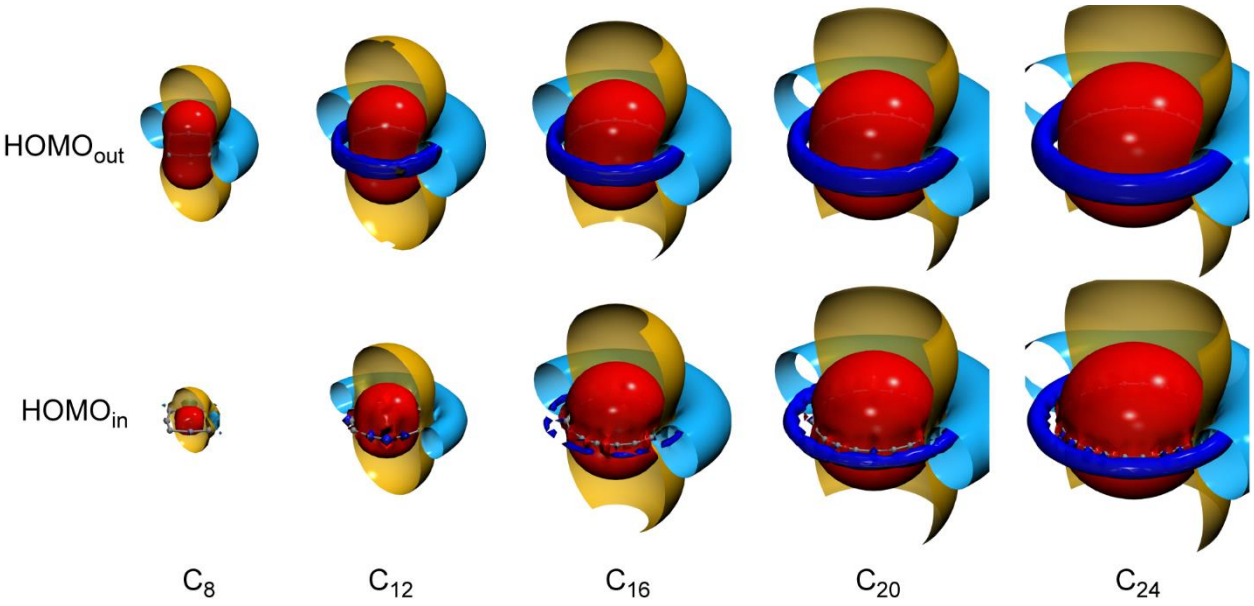

Figure S6. Isosurfaces of $HOMO_{out}$ (top) and $HOMO_{in}$ (bottom) contributions to B_z^{ind} of C_{4n} (n=2-6) rings. Isovalues: cyan -5ppm, orange +5ppm, blue -25ppm, red +25ppm.

References

[1] J. K. Kang, C. B. Musgrave, *J. Chem. Phys.* **2001**, *115*, 11040–11051.

[2] T. Yanai, D. P. Tew, N. C. Handy, *Chem. Phys. Lett.* **2004**, *393*, 51–57.

[3] Y. Zhao, D. G. Truhlar, *J. Phys. Chem. A* **2006**, *110*, 13126–13130.

[4] Y. Zhao, D. G. Truhlar, *Theor. Chem. Acc.* **2008**, *120*, 215–241.

[5] J. Da Chai, M. Head-Gordon, *J. Chem. Phys.* **2008**, *128*, 084106.

[6] A. D. Becke, *Phys. Rev. A* **1988**, *38*, 3098–3100.

[7] J. P. Perdew, J. A. Chevary, S. H. Vosko, K. A. Jackson, M. R. Pederson, D. J. Singh, C. Fiolhais, *Phys. Rev. B* **1992**, *46*, 6671–6687.

[8] P. J. Stephens, F. J. Devlin, C. F. Chabalowski, M. J. Frisch, *J. Phys. Chem.* **1994**, *98*, 11623–11627.

[9] M. Ernzerhof, G. E. Scuseria, *J. Chem. Phys.* **1999**, *110*, 5029–5036.

[10] J. Heyd, G. E. Scuseria, M. Ernzerhof, *J. Chem. Phys.* **2003**, *118*, 8207–8215.

[11] R. Peverati, D. G. Truhlar, *Phys. Chem. Chem. Phys.* **2012**, *14*, 16187–16191.

[12] J. Tao, J. P. Perdew, V. N. Staroverov, G. E. Scuseria, *Phys. Rev. Lett.* **2003**, *91*, 146401.

[13] G. I. Csonka, J. P. Perdew, A. Ruzsinszky, *J. Chem. Theory Comput.* **2010**, *6*, 3688–3703.

Cartesian Coordinates

ωB97XD/6-311++G(d,p)

C_6 *D_{3h}*

E = -228.206530

C	0.0000000	-1.0859440	0.0000000
C	1.2735170	-0.7352820	0.0000000
C	0.9405770	0.5430000	0.0000000
C	0.0000000	1.4705090	0.0000000
C	-0.9405770	0.5430000	0.0000000
C	-1.2735170	-0.7352820	0.0000000

C_8 *C_{4h}*

E = -304.335629

C	-1.3027820	1.3027820	0.0000000
C	-0.0672930	1.4993900	0.0000000
C	0.0672930	-1.4993900	0.0000000
C	1.3027820	1.3027820	0.0000000
C	1.3027820	-1.3027820	0.0000000
C	1.4993900	0.0672930	0.0000000
C	-1.3027820	-1.3027820	0.0000000
C	-1.4993900	-0.0672930	0.0000000

C_{10} *D_{5h}*

E = -380.575446

C	1.2790080	1.7604040	0.0000000
C	0.0000000	1.9283100	0.0000000
C	1.1334320	-1.5600360	0.0000000
C	-1.2790080	1.7604040	0.0000000
C	0.0000000	-2.1759790	0.0000000
C	-1.8339320	0.5958810	0.0000000

C	2.0694790	-0.6724140	0.0000000
C	1.8339320	0.5958810	0.0000000
C	-2.0694790	-0.6724140	0.0000000
C	-1.1334320	-1.5600360	0.0000000

C_{12} *C_{6h}*

E = -456.681834

C	0.0000000	2.5793970	0.0000000
C	1.1280850	2.0803390	0.0000000
C	2.2338240	1.2896990	0.0000000
C	-2.2338240	1.2896990	0.0000000
C	-2.3656690	-0.0632190	0.0000000
C	-2.2338240	-1.2896990	0.0000000
C	2.3656690	0.0632190	0.0000000
C	-1.2375840	2.0171200	0.0000000
C	-1.1280850	-2.0803390	0.0000000
C	2.2338240	-1.2896990	0.0000000
C	1.2375840	-2.0171200	0.0000000
C	0.0000000	-2.5793970	0.0000000

C_{14} *C_{7h}*

E = -532.870509

C	-1.8300790	2.2948460	0.0000000
C	-0.5956820	2.7253300	0.0000000
C	0.6531480	2.8616270	0.0000000
C	-1.8300790	-2.2948460	0.0000000
C	-0.6457850	-2.7138940	0.0000000
C	0.6531480	-2.8616270	0.0000000
C	1.7593470	2.1649390	0.0000000
C	-2.5021510	1.2334920	0.0000000
C	-2.5244480	-1.1871900	0.0000000

C	1.7191680	-2.1969810	0.0000000
C	2.6445410	1.2735440	0.0000000
C	2.7895520	-0.0256960	0.0000000
C	2.6445410	-1.2735440	0.0000000
C	-2.9352190	0.0000000	0.0000000

C_{14} *D_{7h}* TS

E = -532.870323

C	0.6658156	2.8593626	0.0000000
C	-0.6063816	2.7113108	0.0000000
C	-1.8204423	2.3033139	0.0000000
C	-2.4978760	1.2163169	0.0000000
C	-2.9361268	0.0128347	0.0000000
C	-2.5082764	-1.1943892	0.0000000
C	-1.8404759	-2.2872995	0.0000000
C	-0.6300058	-2.7058595	0.0000000
C	0.6408267	-2.8653253	0.0000000
C	1.7226534	-2.1796900	0.0000000
C	2.6394969	-1.2853588	0.0000000
C	2.7781054	-0.0120959	0.0000000
C	2.6509281	1.2623731	0.0000000
C	1.7417588	2.1645063	0.0000000

C_{16} *C_{8h}*

E = -609.001310

C	-0.0754360	3.2966470	0.0000000
C	1.2679410	3.0610800	0.0000000
C	2.2777400	2.3844230	0.0000000
C	3.0610800	1.2679410	0.0000000
C	3.2966470	0.0754360	0.0000000
C	3.0610800	-1.2679410	0.0000000
C	2.3844230	-2.2777400	0.0000000

C	1.2679410	-3.0610800	0.0000000
C	0.0754360	-3.2966470	0.0000000
C	-1.2679410	-3.0610800	0.0000000
C	-2.2777400	-2.3844230	0.0000000
C	-1.2679410	3.0610800	0.0000000
C	-3.0610800	1.2679410	0.0000000
C	-2.3844230	2.2777400	0.0000000
C	-3.0610800	-1.2679410	0.0000000
C	-3.2966470	-0.0754360	0.0000000

C_{18} *C_{9h}*

E = -685.16711831

C	1.8496640	3.2037110	0.0000000
C	0.5804130	3.6511990	0.0000000
C	-0.6423810	3.6431260	0.0000000
C	-1.9023230	3.1700630	0.0000000
C	-2.8338490	2.3778820	0.0000000
C	-3.4949410	1.2056190	0.0000000
C	-3.6993270	0.0000000	0.0000000
C	-3.4522370	-1.3229470	0.0000000
C	-2.8338490	-2.3778820	0.0000000
C	-1.7941930	-3.2324920	0.0000000
C	-0.6423810	-3.6431260	0.0000000
C	0.7033740	-3.6295180	0.0000000
C	1.8496640	-3.2037110	0.0000000
C	2.8718250	-2.3282520	0.0000000
C	3.4762300	-1.2652440	0.0000000
C	3.6965170	0.0624290	0.0000000
C	3.4762300	1.2652440	0.0000000
C	2.7915680	2.4238980	0.0000000

C_{18} *D_{9h}* TS

E = -685.14975271

C	0.0000000	3.6131830	0.0000000
C	1.2718520	3.4943840	0.0000000
C	2.3225090	2.7678590	0.0000000
C	3.2204420	1.8593230	0.0000000
C	3.5582900	0.6274230	0.0000000
C	3.6621510	-0.6457360	0.0000000
C	3.1291080	-1.8065910	0.0000000
C	2.3902990	-2.8486480	0.0000000
C	1.2357810	-3.3952810	0.0000000
C	0.0000000	-3.7186460	0.0000000
C	-1.2357810	-3.3952810	0.0000000
C	-2.3902990	-2.8486480	0.0000000
C	-3.1291080	-1.8065910	0.0000000
C	-3.6621510	-0.6457360	0.0000000
C	-3.5582900	0.6274230	0.0000000
C	-3.2204420	1.8593230	0.0000000
C	-2.3225090	2.7678590	0.0000000
C	-1.2718520	3.4943840	0.0000000

C_{20} *C_{10h}*

E = -761.308249

C	1.20382200	3.93675000	0.00000000
C	0.00000000	4.10985900	0.00000000
C	-1.34005100	3.89248700	0.00000000
C	-2.41571500	3.32494600	0.00000000

C	-3.37207000	2.36142600	0.00000000
C	-3.90870800	1.27001600	0.00000000
C	-4.11607400	-0.07162000	0.00000000
C	-3.90870800	-1.27001600	0.00000000
C	-3.28787700	-2.47730900	0.00000000
C	-2.41571500	-3.32494600	0.00000000
C	-1.20382200	-3.93675000	0.00000000
C	0.00000000	-4.10985900	0.00000000
C	1.34005100	-3.89248700	0.00000000
C	2.41571500	-3.32494600	0.00000000
C	3.37207000	-2.36142600	0.00000000
C	3.90870800	-1.27001600	0.00000000
C	4.11607400	0.07162000	0.00000000
C	3.90870800	1.27001600	0.00000000
C	3.28787700	2.47730900	0.00000000
C	2.41571500	3.32494600	0.00000000

C_{22} *C_{11h}*

E = -837.462203

C	0.57579800	4.47169300	0.00000000
C	-0.64304500	4.47247600	0.00000000
C	-1.93318700	4.07312800	0.00000000
C	-2.95896700	3.41483000	0.00000000
C	-3.82840000	2.38137300	0.00000000
C	-4.33543800	1.27299900	0.00000000
C	-4.50812200	-0.06645100	0.00000000
C	-4.33543800	-1.27299900	0.00000000
C	-3.75654800	-2.49317700	0.00000000

C	-2.95896700	-3.41483000	0.00000000
C	-1.81229600	-4.12833700	0.00000000
C	-0.64304500	-4.47247600	0.00000000
C	0.70734700	-4.45277900	0.00000000
C	1.87703900	-4.11014300	0.00000000
C	3.00241200	-3.36349500	0.00000000
C	3.80117700	-2.44286800	0.00000000
C	4.34423300	-1.20632600	0.00000000
C	4.51846800	0.00000000	0.00000000
C	4.30679000	1.33384400	0.00000000
C	3.80117700	2.44286800	0.00000000
C	2.90197200	3.45052700	0.00000000
C	1.87703900	4.11014300	0.00000000

C_{22} *D_{11h}* TS

E = -837.423290

C	0.00000000	4.43090000	0.00000000
C	-1.27217100	4.33124200	0.00000000
C	-2.39672700	3.72824700	0.00000000
C	-3.41334600	2.95701900	0.00000000
C	-4.03352400	1.84183700	0.00000000
C	-4.47118600	0.64316600	0.00000000
C	-4.38871200	-0.63021800	0.00000000
C	-4.10813600	-1.87505100	0.00000000
C	-3.35039500	-2.90174300	0.00000000
C	-2.44148800	-3.79740700	0.00000000
C	-1.24893300	-4.25141800	0.00000000
C	-0.00016200	-4.51360400	0.00000000

C	1.24876100	-4.25179400	0.00000000
C	2.44121600	-3.79770100	0.00000000
C	3.35061200	-2.90249600	0.00000000
C	4.10870700	-1.87606900	0.00000000
C	4.38918900	-0.63118800	0.00000000
C	4.47158500	0.64222100	0.00000000
C	4.03328600	1.84065400	0.00000000
C	3.41287700	2.95571400	0.00000000
C	2.39648400	3.72718000	0.00000000
C	1.27206400	4.33050900	0.00000000

C_{24} *C_{12h}*

E = -913.605670

C	4.89181400	0.60809900	0.00000000
C	4.53213800	1.91472200	0.00000000
C	3.93226300	2.97256700	0.00000000
C	2.96761000	3.92439700	0.00000000
C	1.91930400	4.54089500	0.00000000
C	0.60806600	4.88299300	0.00000000
C	-0.60806700	4.89239300	0.00000000
C	-1.91448100	4.53243300	0.00000000
C	-2.97226900	3.93237700	0.00000000
C	-3.92397300	2.96763900	0.00000000
C	-4.54042200	1.91929200	0.00000000
C	-4.88252100	0.60806200	0.00000000
C	-4.89198100	-0.60807400	0.00000000
C	-4.53213200	-1.91451700	0.00000000
C	-3.93218600	-2.97236800	0.00000000

C	-2.96755500	-3.92418100	0.00000000
C	-1.91927200	-4.54073600	0.00000000
C	-0.60806700	-4.88294000	0.00000000
C	0.60806600	-4.89245000	0.00000000
C	1.91451300	-4.53259500	0.00000000
C	2.97232100	-3.93259300	0.00000000
C	3.92404500	-2.96783400	0.00000000
C	4.54042400	-1.91949400	0.00000000
C	4.88235900	-0.60808800	0.00000000

C_{26} *C_{13h}*

E = -989.753925

C	3.99206500	3.53666100	0.00000000
C	0.57416600	5.29264100	0.00000000
C	5.17836600	1.27635300	0.00000000
C	4.68192200	2.53403300	0.00000000
C	1.89123000	-4.98676300	0.00000000
C	3.07990100	-4.34234100	0.00000000
C	3.99206500	-3.53666100	0.00000000
C	4.74510300	-2.41365100	0.00000000
C	5.17836600	-1.27635300	0.00000000
C	5.32326000	0.06797800	0.00000000
C	-0.64286400	5.29445700	0.00000000
C	-1.95121400	4.95322900	0.00000000
C	-3.02968400	4.38925600	0.00000000
C	-4.02959500	3.47909200	0.00000000
C	-3.02968400	-4.38925600	0.00000000
C	-1.82409400	-5.00144000	0.00000000

C	0.70913000	-5.27625300	0.00000000
C	-0.64286400	-5.29445700	0.00000000
C	-5.15230700	-1.33994200	0.00000000
C	-5.33334400	0.00000000	0.00000000
C	-5.18484400	1.20793700	0.00000000
C	-4.72244100	2.47852800	0.00000000
C	1.89123000	4.98676300	0.00000000
C	2.96801200	4.41957300	0.00000000
C	-4.72244100	-2.47852800	0.00000000
C	-3.93944000	-3.58085600	0.00000000

C_{26} *D_{13h}* TS

E = -989.694306

C	0.5993758	5.2117963	-0.0006111
C	-0.6746203	5.2759736	-0.0002328
C	-1.8913579	4.8929044	-0.0011626
C	-3.0494916	4.3581542	-0.0006488
C	-3.9490533	3.4537415	-0.0013906
C	-4.7262489	2.4422245	-0.0006315
C	-5.1021778	1.2232467	-0.0011087
C	-5.3195518	-0.0337151	-0.0005291
C	-5.0855967	-1.2877024	-0.0011518
C	-4.6938637	-2.5016727	-0.0001669
C	-3.9040811	-3.5034083	-0.0006701
C	-2.9933723	-4.3966039	0.0003747
C	-1.8287873	-4.9171590	0.0000369
C	-0.6073461	-5.2850130	0.0008381
C	0.6657340	-5.2045071	0.0002194

C	1.9181889	-4.9624736	0.0012008
C	3.0077169	-4.2990405	0.0007121
C	4.0038606	-3.5022292	0.0014816
C	4.6602888	-2.4084696	0.0007135
C	5.1720898	-1.2400131	0.0012604
C	5.2452476	0.0334994	0.0002136
C	5.1560467	1.3059843	0.0008703
C	4.6295338	2.4678612	-0.0000648
C	3.9594702	3.5533171	0.0005358
C	2.9531346	4.3372228	-0.0003708
C	1.8548609	4.9860813	0.0002822

C_{28} *C_{14h}*

E = -1065.897865

C	0.01166100	-0.02217400	0.00000000
C	1.22772100	-0.01900200	0.00000000
C	2.54222200	0.30471700	0.00000000
C	3.63665400	0.83482400	0.00000000
C	4.68019000	1.69715000	0.00000000
C	5.43648900	2.64941000	0.00000000
C	6.00280100	3.87898200	0.00000000
C	6.26968900	5.06538600	0.00000000
C	6.24506600	6.41890900	0.00000000
C	5.97094700	7.60365300	0.00000000
C	5.36104500	8.81219500	0.00000000
C	4.59933700	9.76013400	0.00000000
C	3.52562800	10.58465100	0.00000000
C	2.42828100	11.10868500	0.00000000
C	1.10320600	11.38586500	0.00000000

C	-0.11285400	11.38269300	0.00000000
C	-1.42735400	11.05897400	0.00000000
C	-2.52178600	10.52886700	0.00000000
C	-3.56532200	9.66654000	0.00000000
C	-4.32162200	8.71428100	0.00000000
C	-4.88793400	7.48470800	0.00000000
C	-5.15482200	6.29830500	0.00000000
C	-5.13019900	4.94478200	0.00000000
C	-4.85608000	3.76003700	0.00000000
C	-4.24617700	2.55149600	0.00000000
C	-3.48447000	1.60355700	0.00000000
C	-2.41076000	0.77904000	0.00000000
C	-1.31341400	0.25500600	0.00000000